Crown-containing butadienyl dyes
1. Synthesis, structure, fluorescence, and complex formation of chromogenic aza-15-crown-5 ethers

S. P. Gromov,[a*] *S. A. Sergeev,*[a] *S. I. Druzhinin,*[b] *M. V. Rusalov,*[b] *B. M. Uzhinov,*[b] *L. G. Kuz'mina,*[c] *A. V. Churakov,*[c] *J. A. K. Howard,*[d] *and M. V. Alfimov*[a]

[a]*Photochemistry Center of Russian Academy of Sciences,*
7A ul. Novatorov, 117421 Moscow, Russian Federation.
Fax: +7 (095) 936 1255. E-mail: gromov@mx.icp.rssi.ru
[b]*Chemistry Department, M. V. Lomonosov Moscow State University,*
Leninskie Gory, 119899 Moscow, Russian Federation.
Fax: +7 (095) 932 8846. E-mail: druzh@light.chem.msu.su
[c]*N. S. Kurnakov Institute of General and Inorganic Chemistry of Russian Academy of Sciences,*
31 Leninsky prosp., 117907 Moscow, Russian Federation.
Fax: +7 (095) 954 1279. E-mail: kuzmina@ionchran.msk.ru
[d]*Crystallographic Centre, Department of Chemistry, University of Durham,*
South Road, DH1 3LE, Durham, UK.
Fax: +44 (191) 374 3745. E-mail: J.A.K.Howard@durham.ac.uk

Crown-containing butadienyl dyes containing various heterocyclic moieties and azacrown ether fragments were synthesized for the first time. The spatial structures and the absorption and fluorescence spectra of crown-containing butadienyl dyes and their complexes with metal cations were examined. The effects of the nature of the heterocyclic and crown ether fragments on fluorescence and generation of dyes and their complexes with metal cations were revealed based on the spectral data.

Key words: crown-containing butadienyl dyes; synthesis; X-ray diffraction analysis; fluorescence; complex formation.

Photostructural conversions of crown-containing styryl dyes (CSD) lead to a change in the efficiency of binding of metal cations with a fragment of the crown compound. Complexation, in turn, changes the spectral and photochemical characteristics of the dye fragment.[1,2] Coupled reactions of this type can be used for developing and constructing previously unknown types of molecular photochemical and photophysical devices.[3] It may be that readily accessible selective irradiation with light is the most promising way of controlling these devices. Recently, we have demonstrated that CSD complexes with metal ions can undergo photoinduced recoordination.[4,5] This unusual behavior of CSD is characterized by the fact that the fluorescence maximum, unlike the maximum of the absorption spectrum, changes only slightly upon addition of metal salts. The reaction mechanism lies in the fact that in the excited state of the CSD complex the coordination bond between the metal cation and the heteroatom of the macrocycle that is bound with the π-conjugated system of the dye is cleaved. Using the complex of *trans*-**1** with Ca^{2+} as an example, we have observed the recoordination reaction not only in the excited but also in the ground state.[6]

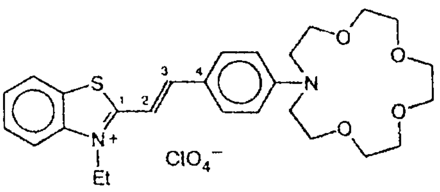

trans-**1**

However, the quantum yields of fluorescence of *trans* isomers of CSD in low-viscosity solvents at room temperature are low.[4,6,7] In addition, these dyes in the excited state undergo efficient *trans—cis* isomerization and structural relaxation (see, for example, Ref. 8).

It is known that the quantum yield of fluorescence increases by approximately an order of magnitude when the conjugation chain length in polymethine dyes increases from $n = 1$ to $n = 2$.[9] Actually, butadienyl dyes exhibit rather efficient fluorescence and can generate laser radiation upon pulse excitation.[10,11] Crown-containing butadienyl dyes (CBD) have not yet been reported. It was of interest to develop a procedure for the synthesis and to study the structures, fluorescence, com-

---

Translated from *Izvestiya Akademii Nauk. Seriya Khimicheskaya,* No. 3, pp. 530—541, March, 1999.

plex formation, and the generating properties of a new type of polymethine dyes containing two double bonds and the crown ether fragment.

Synthesis of crown-containing butadienyl dyes

For this purpose, we synthesized dyes **2a,b,d** containing the phenylaza-15(18)-crown-5(6) ether fragments as well as dyes **2c,e** containing the dimethylamino group, which simulates on the whole the electron-donating effect of the azacrown ether fragment. Unlike compounds **2a,b,d**, compounds **2c,e** should not be able to form complexes with metal cations in noticeable yields.

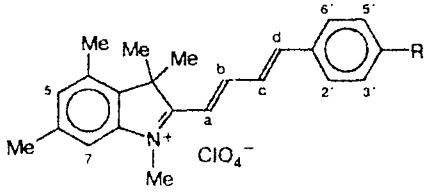

trans,trans-**2a—c**

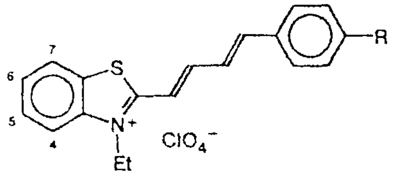

trans,trans-**2d,e**

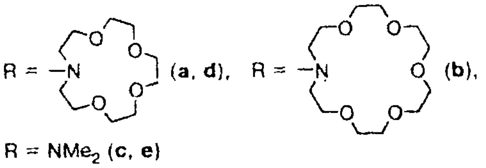

Hexamethylindoleninium perchlorate (**3a**) was prepared by a two-stage procedure from 1,2,4,6-tetramethyl-3-nitropyridinium iodide (**4**) using a new method for the synthesis of indoles, which we have developed previously (Scheme 1).[12,13] The quaternary salt (**3b**) was prepared by adding an excess of perchloric acid to an alcoholic solution of 3-ethyl-2-methylbenzothiazolium iodide.[8] *N*-Methyl-*N*-phenylaminoacrolein (**5**), which is required for the synthesis of crown-containing aldehydes, was prepared in two stages from propargyl alcohol according to known procedures.[14,15]

Crown-containing cinnamaldehydes (**6a,b**) were not described in the literature. We have developed a procedure for the synthesis of these compounds, which is based on the Vilsmeier reaction with the use of vinylog **5** instead of *N*-methyl-*N*-phenylformamide. Aldehydes **6a,b** were prepared by the reaction of *N*-phenylazacrown ethers (**7a,b**) with *N*-methyl-*N*-phenylaminoacrolein (**5**) under the action of $POCl_3$ in anhydrous THF at −10 °C in yields of up to 37%. Dimethylaminocinnamaldehyde (**6c**) was prepared analogously from *N,N*-dimethylaniline (**7c**) in 47% yield.

Scheme 1

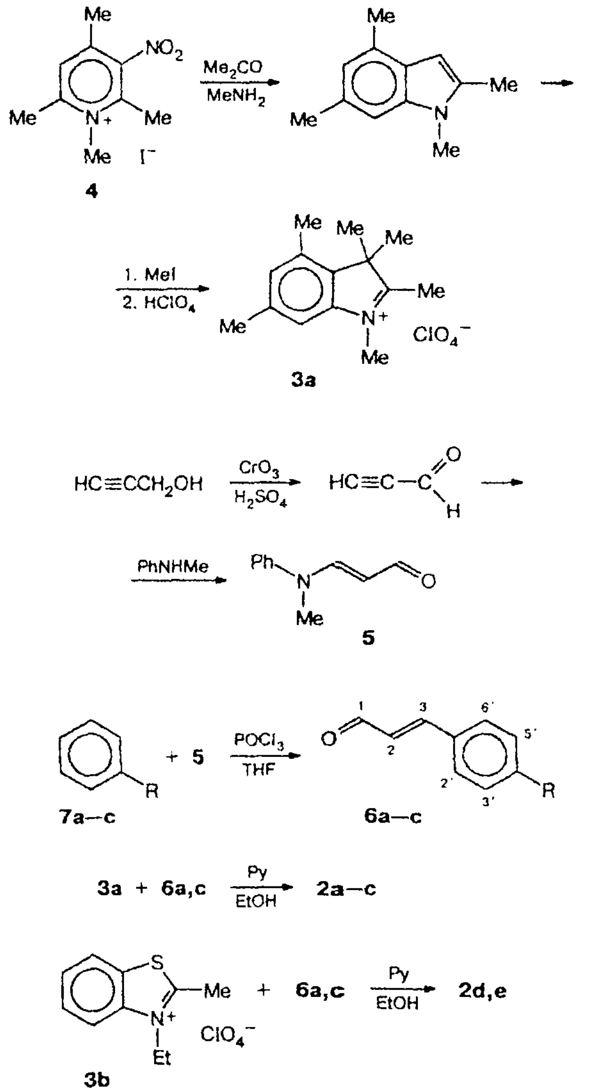

Butadienyl dyes **2a—e** were synthesized by condensation of cinnamaldehydes **6a—c** with quaternary salts **3a,b** upon boiling in alcohol in the presence of pyridine as a base in yields of up to 74%.

Structures of crown-containing butadienyl dyes

The structures of compounds **2a—e** and **6a—c** were established by ^1H NMR spectroscopy. The structures of compounds **6a,b** were studied also by IR and UV spectroscopy and mass spectrometry. The data of elemental analysis correspond to the structures proposed (Tables 1 and 2).

The assignment of the signals in the ^1H NMR spectra of crown-containing butadienyl dye **2d** was made

Table 1. Characteristics of aldehydes **6a—c** and crown-containing butadienyl dyes *trans,trans*-**2a—e**

Compound	M.p.[a]/°C	Yield (%)	Found / Calculated (%) C	H	N	Molecular formula
2a	197—198	74	62.34 62.63	7.11 7.17	4.47 4.43	$C_{33}H_{45}ClN_2O_8$
2b	229—230	68	61.77 62.10	7.24 7.30	3.92 4.14	$C_{35}H_{49}ClN_2O_9$
2c	254—255	38	65.49 65.47	6.79 6.82	6.07 6.11	$C_{25}H_{31}ClN_2O_4$
2d	206—208	66	56.76 57.22	6.16 6.13	4.36 4.60	$C_{29}H_{37}ClN_2O_8S$
2e	266—268	62	58.01 58.05	5.27 5.34	6.97 6.45	$C_{21}H_{23}ClN_2O_4S$
6a	101—102	37	65.23 65.31	7.91 7.79	3.79 4.01	$C_{19}H_{27}NO_5$
6b	72—73	35	64.07 64.10	8.20 7.94	3.32 3.56	$C_{21}H_{31}NO_6$
6c	141—142[b]	47	—	—	—	$C_{11}H_{13}NO$

[a] M.p. of **2a—e** from EtOH. [b] *Cf.* Ref. 15.

Table 2. ^{1}H NMR spectra of aldehydes **6a—c** and crown-containing butadienyl dyes *trans,trans*-**2a—e**

Compound	^{1}H NMR (DMSO-d$_6$), δ (*J*/Hz)
2a	1.75 (s, 6 H, CMe$_2$); 2.41 (s, 3 H, Me); 2.50 (s, 3 H, Me); 3.53—3.74 (m, 20 H, 8 CH$_2$O, 2 CH$_2$N); 3.88 (s, 3 H, NMe); 6.83 (m, 2 H, HC(3´), HC(5´)); 6.92 (d, 1 H, HC$_a$, J_{H_a,H_b} = 15.0); 7.11, 7.41 (both s, 2 H, HC(5), HC(7)); 7.23 (dd, 1 H, HC$_c$, J_{H_c,H_d} = 14.8, J_{H_c,H_b} = 11.0); 7.57 (m, 2 H, HC(2´), HC(6´)); 7.66 (d, 1 H, HC$_d$, J_{H_d,H_c} = 14.8); 8.23 (dd, 1 H, HC$_b$, J_{H_b,H_a} = 15.0, J_{H_b,H_c} = 11.0)
2b	1.73 (s, 6 H, CMe$_2$); 2.34 (s, 3 H, Me); 2.60 (s, 3 H, Me); 3.58—3.70 (m, 24 H, 10 CH$_2$O, 2 CH$_2$N); 4.12 (s, 3 H, NMe); 6.86 (m, 2 H, HC(3´), HC(5´)); 6.91 (d, 1 H, HC$_a$, J_{H_a,H_b} = 15.0); 7.12, 7.39 (both s, 2 H, HC(5), HC(7)); 7.24 (dd, 1 H, HC$_c$, J_{H_c,H_d} = 14.8, J_{H_c,H_b} = 11.0); 7.56 (m, 2 H, HC(2´), HC(6´)); 7.62 (d, 1 H, HC$_d$, J_{H_d,H_c} = 14.8); 8.17 (dd, 1 H, HC$_b$, J_{H_b,H_a} = 15.0, J_{H_b,H_c} = 11.0)
2c	1.83 (s, 6 H, 2 CMe$_2$); 2.49 (s, 3 H, Me); 2.60 (s, 3 H, Me); 3.17 (s, 6 H, NMe$_2$); 3.95 (s, 3 H, NMe); 6.92 (m, 2 H, HC(3´), HC(5´)); 7.02 (d, 1 H, HC$_a$, J_{H_a,H_b} = 15.0); 7.35 (dd, 1 H, HC$_c$, J_{H_c,H_d} = 14.7, J_{H_c,H_b} = 11.3); 7.20, 7.53 (both s, 2 H, HC(5), HC(7)); 7.68 (m, 2 H, HC(2´), HC(6´)); 7.78 (d, 1 H, HC$_d$, J_{H_d,H_c} = 14.7); 8.35 (dd, 1 H, HC$_b$, J_{H_b,H_a} = 15.0, J_{H_b,H_c} = 11.3)
2d	1.49 (t, 3 H, Me, *J* = 7.1); 3.53—3.77 (m, 20 H, 8 CH$_2$O, 2 CH$_2$N); 4.74 (q, 2 H, CH$_2$N, *J* = 7.1); 6.81 (m, 2 H, HC(3´), HC(5´)); 7.19 (dd, 1 H, HC$_c$, J_{H_c,H_d} = 15.0, J_{H_c,H_b} = 10.7); 7.32 (d, 1 H, HC$_a$, J_{H_a,H_b} = 14.5); 7.45 (d, 1 H, HC$_d$, J_{H_d,H_c} = 15.0); 7.53 (m, 2 H, HC(2´), HC(6´)); 7.71, 7.81 (both m, 2 H, HC(5), HC(6)); 7.98 (dd, 1 H, HC$_b$, J_{H_b,H_a} = 14.5, J_{H_b,H_c} = 10.7); 8.14, 8.30 (both d, 2 H, HC(7) and HC(4), *J* = 7.8 and *J* = 8.0)
2e	1.53 (t, 3 H, Me, *J* = 7.2); 3.13 (s, 6 H, NMe$_2$); 4.81 (q, 2 H, CH$_2$N, *J* = 7.2); 6.87 (m, 2 H, HC(3´), HC(5´)); 7.30 (dd, 1 H, HC$_c$, J_{H_c,H_d} = 15.0, J_{H_c,H_b} = 11.1); 7.42 (d, 1 H, HC$_a$, J_{H_a,H_b} = 14.4); 7.54 (d, 1 H, HC$_d$, J_{H_d,H_c} = 15.0); 7.62 (m, 2 H, HC(2´), HC(6´)); 7.80, 7.89 (both m, 2 H, HC(5), HC(6)); 8.08 (dd, 1 H, HC$_b$, J_{H_b,H_a} = 14.4, J_{H_b,H_c} = 11.1); 8.26, 8.42 (both d, 2 H, HC(7), HC(4), *J* = 8.4 and *J* = 8.0)
6a*	3.66—3.80 (m, 20 H, 8 CH$_2$O, 2 CH$_2$N); 6.54 (dd, 1 H, HC(2), $J_{H(2),H(3)}$ = 15.7, $J_{H(2),H(1)}$ = 7.9); 6.69 (m, 2 H, HC(3´), HC(5´)); 7.38 (d, 1 H, HC(3), $J_{H(3),H(2)}$ = 15.7); 7.44 (m, 2 H, HC(2´), HC(6´)); 9.60 (d, 1 H, CHO, $J_{H(1),H(2)}$ = 7.9)
6b*	3.67—3.74 (m, 24 H, 10 CH$_2$O, 2 CH$_2$N); 6.54 (dd, 1 H, HC(2), $J_{H(2),H(3)}$ = 15.6, $J_{H(2),H(1)}$ = 7.8); 6.72 (m, 2 H, HC(3´), HC(5´)); 7.37 (d, 1 H, HC(3), $J_{H(3),H(2)}$ = 15.7); 7.43 (m, 2 H, HC(2´), HC(6´)); 9.60 (d, 1 H, CHO, $J_{H(1),H(2)}$ = 7.8)
6c*	3.06 (s, 6 H, NMe$_2$); 6.52 (dd, 1 H, HC(2), $J_{H(2),H(3)}$ = 15.7, $J_{H(2),H(1)}$ = 7.7); 6.66 (m, 2 H, HC(3´), HC(5´)); 7.34 (d, 1 H, HC(3), $J_{H(3),H(2)}$ = 15.7); 7.42 (m, 2 H, HC(2´), HC(6´)); 9.58 (d, 1 H, CHO, $J_{H(1),H(2)}$ = 7.7)

* The ^{1}H NMR spectrum was obtained in CDCl$_3$.

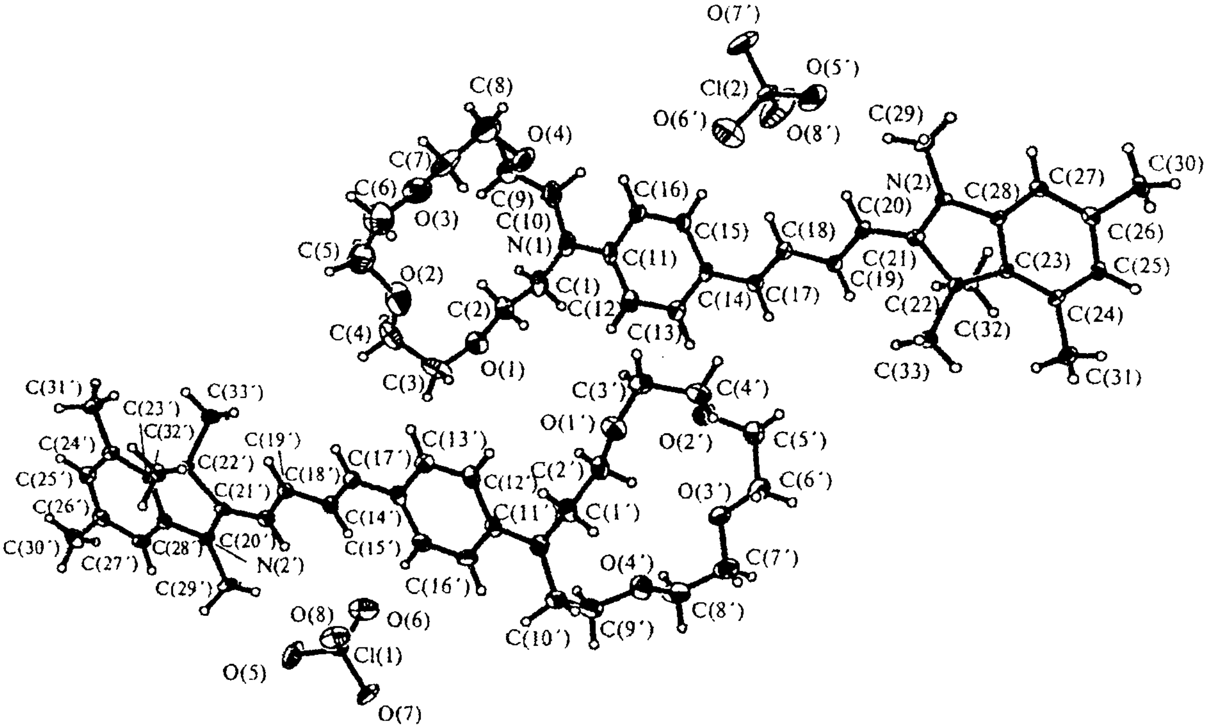

Fig. 1. Structures of the crystallographically independent structural units of *trans,trans*-**2a**. The atoms of *trans,trans*-**2a** are represented as ellipsoids of the root-mean-square thermal displacements calculated with 0.5 probability. The atomic numbering schemes for organic cations **A** (nonprimed) and **B** (primed) are identical.

based on the data of COSY spectroscopy. The values of the spin-spin coupling constants for the olefin protons ($^3J_{trans}$ = 15.6—15.7 Hz) indicate that synthesized aldehydes **6a—c** exist in the *trans* form. All butadienyl dyes **2a—e** have a *trans,trans* configuration ($^3J_{H_a,H_b}$ and $^3J_{H_c,H_d}$ = 14.4—15.0 Hz) and an *s-trans* conformation ($^3J_{H_b,H_c}$ = 10.7—11.3 Hz).

A knowledge of the three-dimensional structures of CBD molecules is necessary for an understanding of the character of interactions between the chromogenic and crown ether moieties of the compounds synthesized. Presently, X-ray diffraction analysis is the unique method, which allows one to obtain precise data on configurations and molecular conformations. Therefore, in this work we report for the first time the results of X-ray diffraction study of chromogenic azacrown ether **2a** of the butadienyl series.

There are two crystallographically independent structural units of compound **2a** (two organic cations, **A** and **B**, and two perchlorate anions) per asymmetric unit. The structures of these units and the atomic numbering scheme are shown in Fig. 1. The bond lengths and bond angles are given in Tables 3 and 4, respectively. The coordinates of nonhydrogen atoms are listed in Table 5.

Two independent organic cations differ substantially only by the spatial structures of the azacrown ether fragments. The corresponding geometric parameters of the two aromatic systems (the benzene and indolenine fragments) and the diene chain between these aromatic systems in cations **A** and **B** coincide to within 1—2 standard deviations.

In both organic cations, five planar fragments can be distinguished, namely, the indoleninium residue N(2)C(21)...C(28) (plane *1*), the double bond C(18)C(19)=C(20)C(21) (plane *2*), the double bond C(14)C(17)=C(18)C(19) (plane *3*), the benzene ring C(11)...C(16) (plane *4*), and the system of the bonds at the N(1) atom (plane *5*). The dihedral angles between the planes *1*/*2*, *2*/*3*, *3*/*4*, and *4*/*5* are 4.0, 3.1, 12.4, and 12.6° in cation **A** and 4.4, 2.3, 11.2, and 7.7° in cation **B**, respectively. Therefore, crown-containing butadienyl dye *trans,trans*-**2a** is characterized by the planar molecular structure due apparently to substantial conjugation between the p-orbitals of the atoms of the indoleninium fragment, two ethylene bonds, the carbon atoms of the benzene ring, and the nitrogen atom of the azacrown ether fragment. In this conjugated system, the bond lengths in the diene fragment alternate only slightly. The formally double C(17)—C(18) (1.358(7) and 1.361(7) Å) and C(19)—C(20) (1.368(7) and 1.380(7) Å) bonds are noticeably longer than those usually observed in C=C—C(Ar) systems (1.339(11) Å), while the formally single C(14)—C(17) (1.450(6) and 1.445(7) Å), C(18)—C(19) (1.418(7) and 1.419(6) Å), and C(20)—C(21) (1.409(6) and 1.401(6) Å) bonds are shorter than those typical of the conjugated C(sp^2)—C(sp^2) system (1.455(11) Å).[16] Previously, we

Table 3. Bond lengths (*d*) in cations **A** and **B** of *trans,trans*-**2a** and in two independent $\mathrm{ClO_4^-}$ anions

Bond	*d*/Å	Bond	*d*/Å	Bond	*d*/Å	Bond	*d*/Å
Cation **A**		Cation **B**					
O(1)—C(2)	1.425(6)	O(1′)—C(2′)	1.420(6)	C(14)—C(17)	1.450(6)	C(14′)—C(17′)	1.445(7)
O(1)—C(3)	1.460(7)	O(1′)—C(3′)	1.413(7)	C(15)—C(16)	1.373(7)	C(15′)—C(16′)	1.375(7)
O(2)—C(4)	1.424(8)	O(2′)—C(4′)	1.423(6)	C(17)—C(18)	1.358(7)	C(17′)—C(18′)	1.361(7)
O(2)—C(5)	1.452(9)	O(2′)—C(5′)	1.420(7)	C(18)—C(19)	1.418(6)	C(18′)—C(19′)	1.419(6)
O(3)—C(6)	1.378(9)	O(3′)—C(6′)	1.409(7)	C(19)—C(20)	1.368(7)	C(19′)—C(20′)	1.380(7)
O(3)—C(7)	1.375(8)	O(3′)—C(7′)	1.408(7)	C(20)—C(21)	1.409(6)	C(20′)—C(21′)	1.401(6)
O(4)—C(8)	1.409(8)	O(4′)—C(8′)	1.421(7)	C(21)—C(22)	1.538(6)	C(21′)—C(22′)	1.524(6)
O(4)—C(9)	1.410(7)	O(4′)—C(9′)	1.427(7)	C(22)—C(23)	1.516(6)	C(22′)—C(23′)	1.523(6)
N(1)—C(11)	1.376(6)	N(1′)—C(11′)	1.380(6)	C(22)—C(32)	1.549(6)	C(22′)—C(32′)	1.562(6)
N(1)—C(1)	1.441(7)	N(1′)—C(1′)	1.456(7)	C(22)—C(33)	1.541(6)	C(22′)—C(33′)	1.538(6)
N(1)—C(10)	1.447(8)	N(1′)—C(10′)	1.472(7)	C(23)—C(24)	1.398(6)	C(23′)—C(24′)	1.388(6)
N(2)—C(21)	1.327(6)	N(2′)—C(21′)	1.331(6)	C(23)—C(28)	1.393(6)	C(23′)—C(28′)	1.392(6)
N(2)—C(28)	1.412(6)	N(2′)—C(28′)	1.415(6)	C(24)—C(25)	1.408(6)	C(24′)—C(25′)	1.401(6)
N(2)—C(29)	1.473(5)	N(2′)—C(29′)	1.479(5)	C(24)—C(31)	1.513(6)	C(24′)—C(31′)	1.514(6)
C(1)—C(2)	1.517(7)	C(1′)—C(2′)	1.528(7)	C(25)—C(26)	1.401(6)	C(25′)—C(26′)	1.393(7)
C(3)—C(4)	1.50(1)	C(3′)—C(4′)	1.493(8)	C(26)—C(27)	1.399(6)	C(26′)—C(27′)	1.396(7)
C(5)—C(6)	1.49(1)	C(5′)—C(6′)	1.516(8)	C(26)—C(30)	1.505(6)	C(26′)—C(30′)	1.514(6)
C(7)—C(8)	1.490(1)	C(7′)—C(8′)	1.50(1)	C(27)—C(28)	1.384(6)	C(27′)—C(28′)	1.381(6)
C(9)—C(10)	1.476(9)	C(9′)—C(10′)	1.514(8)				
C(11)—C(12)	1.400(7)	C(11′)—C(12′)	1.416(7)	$\mathrm{Cl(1)O_4^-}$		$\mathrm{Cl(2)O_4^-}$	
C(11)—C(16)	1.421(7)	C(11′)—C(16′)	1.418(7)	Cl(1)—O(7)	1.428(4)	Cl(2)—O(7′)	1.410(4)
C(12)—C(13)	1.389(7)	C(12′)—C(13′)	1.388(7)	Cl(1)—O(5)	1.431(4)	Cl(2)—O(8′)	1.412(5)
C(13)—C(14)	1.398(7)	C(13′)—C(14′)	1.395(7)	Cl(1)—O(6)	1.437(4)	Cl(2)—O(5′)	1.418(4)
C(14)—C(15)	1.415(7)	C(14′)—C(15′)	1.412(7)	Cl(1)—O(8)	1.437(4)	Cl(2)—O(6′)	1.465(5)

Table 4. Bond angles (ω) in cations **A** and **B** of *trans,trans*-**2a** and in two independent $\mathrm{ClO_4^-}$ anions

Angle	ω/deg	Angle	ω/deg
Cation **A**		Cation **B**	
C(2)—O(1)—C(3)	114.4(4)	C(2′)—O(1′)—C(3′)	115.4(4)
C(4)—O(2)—C(5)	116.4(6)	C(4′)—O(2′)—C(5′)	114.5(4)
C(7)—O(3)—C(6)	113.2(6)	C(7′)—O(3′)—C(6′)	113.0(5)
C(8)—O(4)—C(9)	113.4(5)	C(8′)—O(4′)—C(9′)	113.2(5)
C(11)—N(1)—C(1)	121.6(5)	C(11′)—N(1′)—C(1′)	119.8(4)
C(11)—N(1)—C(10)	122.7(5)	C(11′)—N(1′)—C(10′)	120.9(4)
C(1)—N(1)—C(10)	115.0(5)	C(1′)—N(1′)—C(10′)	118.9(4)
C(21)—N(2)—C(28)	112.3(4)	C(21′)—N(2′)—C(28′)	112.3(4)
C(21)—N(2)—C(29)	127.6(4)	C(21′)—N(2′)—C(29′)	126.9(4)
C(28)—N(2)—C(29)	120.1(4)	C(28′)—N(2′)—C(29′)	120.8(4)
N(1)—C(1)—C(2)	112.1(4)	N(1′)—C(1′)—C(2′)	113.3(4)
O(1)—C(2)—C(1)	105.8(4)	O(1′)—C(2′)—C(1′)	106.1(4)
O(1)—C(3)—C(4)	113.4(5)	O(1′)—C(3′)—C(4′)	114.1(4)
O(2)—C(4)—C(3)	111.6(5)	O(2′)—C(4′)—C(3′)	109.4(4)
O(2)—C(5)—C(6)	107.9(7)	O(2′)—C(5′)—C(6′)	111.8(5)
O(3)—C(6)—C(5)	111.7(7)	O(3′)—C(6′)—C(5′)	107.5(5)
O(3)—C(7)—C(8)	113.1(6)	O(3′)—C(7′)—C(8′)	109.1(5)
O(4)—C(8)—C(7)	113.1(6)	O(4′)—C(8′)—C(7′)	107.5(5)
O(4)—C(9)—C(10)	107.5(5)	O(4′)—C(9′)—C(10′)	106.7(4)
N(1)—C(10)—C(9)	116.0(5)	N(1′)—C(10′)—C(9′)	114.7(4)
N(1)—C(11)—C(12)	121.5(5)	N(1′)—C(11′)—C(12′)	122.3(5)
N(1)—C(11)—C(16)	121.9(5)	N(1′)—C(11′)—C(16′)	120.8(5)
C(12)—C(11)—C(16)	116.6(4)	C(12′)—C(11′)—C(16′)	116.8(4)
C(13)—C(12)—C(11)	121.2(5)	C(13′)—C(12′)—C(11′)	120.9(5)
C(12)—C(13)—C(14)	122.2(5)	C(12′)—C(13′)—C(14′)	122.3(5)
C(13)—C(14)—C(15)	116.5(4)	C(13′)—C(14′)—C(15′)	116.7(4)
C(13)—C(14)—C(17)	120.0(4)	C(13′)—C(14′)—C(17′)	121.4(5)

(to be continued)

Table 4 (*continued*)

Angle	ω/deg	Angle	ω/deg
Cation **A**		Cation **B**	
C(15)—C(14)—C(17)	123.5(4)	C(15′)—C(14′)—C(17′)	122.0(4)
C(16)—C(15)—C(14)	121.7(5)	C(16′)—C(15′)—C(14′)	122.1(5)
C(15)—C(16)—C(11)	121.6(5)	C(15′)—C(16′)—C(11′)	121.2(5)
C(18)—C(17)—C(14)	125.2(4)	C(18′)—C(17′)—C(14′)	124.4(5)
C(17)—C(18)—C(19)	123.1(4)	C(17′)—C(18′)—C(19′)	123.6(5)
C(20)—C(19)—C(18)	121.9(4)	C(20′)—C(19′)—C(18′)	120.2(4)
C(19)—C(20)—C(21)	127.4(4)	C(19′)—C(20′)—C(21′)	126.5(4)
N(2)—C(21)—C(20)	122.6(4)	N(2′)—C(21′)—C(20′)	122.0(4)
N(2)—C(21)—C(22)	108.8(4)	N(2′)—C(21′)—C(22′)	108.8(4)
C(20)—C(21)—C(22)	128.5(4)	C(20′)—C(21′)—C(22′)	129.2(4)
C(23)—C(22)—C(21)	101.0(3)	C(23′)—C(22′)—C(21′)	101.7(3)
C(23)—C(22)—C(33)	112.8(4)	C(23′)—C(22′)—C(33′)	112.8(4)
C(21)—C(22)—C(33)	113.3(4)	C(21′)—C(22′)—C(33′)	113.2(4)
C(23)—C(22)—C(32)	110.8(3)	C(23′)—C(22′)—C(32′)	109.8(4)
C(21)—C(22)—C(32)	107.1(3)	C(21′)—C(22′)—C(32′)	108.1(4)
C(33)—C(22)—C(32)	111.3(4)	C(33′)—C(22′)—C(32′)	110.8(4)
C(24)—C(23)—C(28)	118.6(4)	C(24′)—C(23′)—C(28′)	118.9(4)
C(22)—C(23)—C(24)	132.5(4)	C(22′)—C(23′)—C(24′)	132.7(4)
C(22)—C(23)—C(28)	109.0(4)	C(22′)—C(23′)—C(28′)	108.4(4)
C(23)—C(24)—C(25)	117.4(4)	C(23′)—C(24′)—C(25′)	117.3(4)
C(23)—C(24)—C(31)	123.5(4)	C(23′)—C(24′)—C(31′)	123.0(4)
C(25)—C(24)—C(31)	119.1(4)	C(25′)—C(24′)—C(31′)	119.7(4)
C(26)—C(25)—C(24)	123.0(4)	C(26′)—C(25′)—C(24′)	123.3(4)
C(25)—C(26)—C(27)	119.4(4)	C(25′)—C(26′)—C(27′)	119.1(4)
C(25)—C(26)—C(30)	120.7(4)	C(25′)—C(26′)—C(30′)	121.0(4)
C(27)—C(26)—C(30)	120.0(4)	C(27′)—C(26′)—C(30′)	119.8(4)
C(28)—C(27)—C(26)	116.9(4)	C(28′)—C(27′)—C(26′)	117.1(4)
C(27)—C(28)—C(23)	124.8(4)	C(27′)—C(28′)—C(23′)	124.3(4)
C(27)—C(28)—N(2)	126.8(4)	C(27′)—C(28′)—N(2′)	127.1(4)
C(23)—C(28)—N(2)	108.3(4)	C(23′)—C(28′)—N(2′)	108.5(4)
$Cl(1)O_4^-$		$Cl(2)O_4^-$	
O(7)—Cl(1)—O(5)	110.1(2)	O(7′)—Cl(2)—O(8′)	114.5(3)
O(7)—Cl(1)—O(6)	110.0(3)	O(7′)—Cl(2)—O(5′)	112.1(3)
O(5)—Cl(1)—O(6)	107.9(3)	O(8′)—Cl(2)—O(5′)	113.2(3)
O(7)—Cl(1)—O(8)	110.5(2)	O(7′)—Cl(2)—O(6′)	105.8(3)
O(5)—Cl(1)—O(8)	109.2(3)	O(8′)—Cl(2)—O(6′)	103.8(4)
O(6)—Cl(1)—O(8)	109.1(3)	O(5′)—Cl(2)—O(6′)	106.4(3)

have performed X-ray diffraction study of crown-containing styryl dye *trans*-**1** containing only one double bond C=C,[17] which allowed us to compare these two dyes. A comparison revealed that the alternation of the bond lengths in the C(1)—C(2)—C(3)—C(4) chain in dye *trans*-**1** is more pronounced (C(1)—C(2), 1.437(3) Å; C(2)—C(3), 1.355(3) Å; and C(3)—C(4), 1.424(3) Å), which is indicative of a decrease in the degree of conjugation in the above-mentioned atomic chain in dye *trans*-**1** compared to that observed in compound *trans,trans*-**2a**. Consequently, one would expect the bathochromic shift of the long-wavelength absorption band for *trans,trans*-**2a** compared to *trans*-**1** (Table 6).

The location of the methyl groups in the benzene ring and the distribution of bond lengths at the formally positively charged N(1) atom are of prime interest for the indoleninium fragment. In some instances, it was difficult to locate the methyl groups in the benzene ring of indole derivatives, which were obtained by the unusual reaction of cyclotransformation of nitropyridinium salts,[12,13] using only ^{1}H NMR spectroscopy. The endocyclic C—N bond lengths are nonequivalent: the N(2)—C(28) bond (1.412(6) and 1.415(6) Å) is substantially longer than the N(2)—C(21) bond (1.327(6) and 1.331(6) Å), which is indicative of localization of the double bond in this fragment. Analogous differences in the lengths of the above-mentioned two bonds are also observed in other indoleninium cations available in the Cambridge Structural Database (CSD, the spring 1997 version, the number of entries is 167797).[18] The remaining bond lengths in the indoleninium fragment have standard values.[18]

The benzene ring C(11)...C(16) is characterized by the noticeable contribution of the paraquinoid structure

Table 5. Coordinates of nonhydrogen atoms (×10^4) and their equivalent isotropic temperature parameters (U_{iso}^{eq}×10^4/Å^2) in cations **A** and **B** of *trans,trans*-**2a** and in two independent ClO_4^- anions

Atom	*x*	*y*	*z*	U_{iso}^{eq}	Atom	*x*	*y*	*z*	U_{iso}^{eq}
		Cation **A**					Cation **B**		
O(1)	1390(4)	7940(2)	−207(2)	35(1)	O(1′)	8384(4)	7126(2)	404(2)	35(1)
O(2)	1989(6)	9442(3)	801(3)	63(1)	O(2′)	7903(4)	6173(2)	−1122(2)	33(1)
O(3)	2691(5)	10670(3)	34(2)	54(1)	O(3′)	7737(4)	4741(2)	−782(2)	37(1)
O(4)	3794(4)	10170(2)	−1358(2)	45(1)	O(4′)	7232(4)	4646(2)	644(2)	37(1)
N(1)	3017(5)	8542(3)	−1708(2)	34(1)	N(1′)	6595(4)	6110(3)	1616(2)	28(1)
N(2)	13754(4)	7614(2)	−3854(2)	16(1)	N(2′)	−3944(4)	7376(2)	3722(2)	18(1)
C(1)	2070(5)	8163(3)	−1314(3)	34(1)	C(1′)	7719(5)	6490(3)	1319(3)	28(1)
C(2)	2455(5)	8303(3)	−530(3)	30(1)	C(2′)	7437(5)	6562(3)	547(3)	28(1)
C(3)	1466(6)	8094(4)	565(3)	43(2)	C(3′)	8249(6)	7311(3)	−280(3)	32(1)
C(4)	988(7)	8872(4)	876(3)	48(2)	C(4′)	8895(6)	6753(3)	−842(3)	33(1)
C(5)	1538(10)	10224(4)	960(4)	65(2)	C(5′)	8463(6)	5536(3)	−1564(3)	38(1)
C(6)	2657(11)	10718(5)	757(4)	76(3)	C(6′)	8898(6)	4924(3)	−1150(3)	38(1)
C(7)	3925(7)	10927(3)	−184(4)	51(2)	C(7′)	7916(8)	4079(3)	−489(3)	47(2)
C(8)	3906(8)	10911(4)	−962(5)	61(2)	C(8′)	6864(8)	4060(3)	65(3)	47(2)
C(9)	2410(6)	9905(4)	−1492(4)	44(2)	C(9′)	6289(6)	4701(3)	1207(3)	33(1)
C(10)	2441(7)	9177(4)	−1989(3)	47(2)	C(10′)	6823(6)	5344(3)	1776(3)	32(1)
C(11)	4292(5)	8246(3)	−1893(2)	25(1)	C(11′)	5403(5)	7662(3)	2007(3)	24(1)
C(12)	4685(5)	7532(3)	−1757(3)	27(1)	C(12′)	5243(5)	7277(3)	1769(3)	24(1)
C(13)	5920(5)	7205(3)	−2000(3)	24(1)	C(13′)	4060(5)	7662(3)	2007(3)	24(1)
C(14)	6859(5)	7580(3)	−2365(2)	19(1)	C(14′)	2977(5)	7312(3)	2299(2)	22(1)
C(15)	6497(5)	8319(3)	−2468(2)	23(1)	C(15′)	3119(5)	6531(3)	2323(3)	24(1)
C(16)	5272(5)	8643(3)	−2234(2)	26(1)	C(16′)	4277(5)	6135(3)	2085(3)	26(1)
C(17)	8125(5)	7210(3)	−2616(2)	20(1)	C(17′)	1759(5)	7726(3)	2550(2)	23(1)
C(18)	9213(5)	7555(3)	−2870(2)	21(1)	C(18′)	577(5)	7399(3)	2736(2)	21(1)
C(19)	10412(5)	7162(3)	−3129(2)	21(1)	C(19′)	−582(5)	7818(3)	3016(2)	21(1)
C(20)	11515(5)	7529(3)	−3358(2)	19(1)	C(20′)	−1721(5)	7446(3)	3219(2)	21(1)
C(21)	12758(4)	7207(2)	−3628(2)	16(1)	C(21′)	−2930(5)	7782(3)	3506(2)	18(1)
C(22)	13179(4)	6367(2)	−3750(2)	16(1)	C(22′)	−3314(5)	8618(3)	3652(2)	17(1)
C(23)	14655(4)	6428(2)	−3988(2)	15(1)	C(23′)	−4786(5)	8578(2)	3911(2)	17(1)
C(24)	15698(5)	5893(2)	−4143(2)	18(1)	C(24′)	−5780(5)	9125(3)	4100(2)	19(1)
C(25)	16959(4)	6145(3)	−4378(2)	18(1)	C(25′)	−7044(5)	8882(3)	4332(2)	21(1)
C(26)	17198(5)	6897(3)	−4465(2)	18(1)	C(26′)	−7340(5)	8127(3)	4375(2)	22(1)
C(27)	16159(5)	7433(3)	−4297(2)	19(1)	C(27′)	−6336(5)	7579(3)	4182(2)	20(1)
C(28)	14927(5)	7176(2)	−4066(2)	17(1)	C(28′)	−5094(5)	9956(3)	4058(3)	25(1)
C(29)	13745(5)	8430(2)	−3893(3)	22(1)	C(29′)	−3943(5)	6552(3)	3741(3)	23(1)
C(30)	18557(5)	7131(3)	−4733(3)	23(1)	C(30′)	−8713(5)	7900(3)	4665(3)	28(1)
C(31)	15557(5)	5076(3)	−4040(3)	25(1)	C(31′)	−5558(5)	9956(3)	4058(3)	25(1)
C(32)	12227(5)	5943(2)	−4362(2)	18(1)	C(32′)	−2333(5)	9033(3)	4266(2)	20(1)
C(33)	13093(5)	6002(3)	−3084(2)	21(1)	C(33′)	−3236(5)	9002(3)	2998(3)	22(1)
		$Cl(1)O_4^-$					$Cl(2)O_4^-$		
Cl(1)	221(1)	5448(1)	3471(1)	20(1)	Cl(2)	9589(1)	9635(1)	−3428(1)	24(1)
O(5)	−915(5)	5646(2)	3924(3)	61(2)	O(5′)	10990(4)	9431(3)	−3548(3)	52(1)
O(6)	−200(5)	5564(2)	2774(2)	52(1)	O(6′)	9315(6)	9529(3)	−2707(3)	71(2)
O(7)	570(4)	4670(2)	3455(2)	38(1)	O(7′)	9371(5)	10413(2)	−3438(3)	58(1)
O(8)	1392(4)	5937(2)	3721(2)	43(1)	O(8′)	8626(6)	9138(3)	−3852(3)	77(2)

Table 6. Spectral characteristics of *trans,trans*-**2a—e** in EtOH and MeCN

Dye	λ_a /nm	$\varepsilon_a \cdot 10^{-3}$ [a]	λ_f /nm	$\varphi_f \cdot 10^{-2}$	$\Delta\nu$[b] /cm^{-1}	Dye	λ_a /nm	$\varepsilon_a \cdot 10^{-3}$ [a]	λ_f /nm	$\varphi_f \cdot 10^{-2}$	$\Delta\nu$[b] /cm^{-1}
2a[c]	602	—	702	9.7	490	**2a**[d]	585	67.3	703	5.0	—
2b[c]	599	—	708	8.7	300	**2b**[d]	588	72.8	704	4.6	—
2c[c]	605	—	701	3.7	550	**2c**[d]	585	64.4	702	1.4	—
2d[c]	568	—	705	10.3	250	**2d**[d]	560	63.2	708	5.4	—
2e[c]	571	—	703	5.2	540	**2e**[d]	554	55.9	707	1.6	—
						1[d,e]	522	68.0	600		

[a] ε_a/L mol^{-1} cm^{-1}. [b] $\Delta\nu = \nu_a^{MeCN} - \nu_a^{EtOH}$. [c] In EtOH. [d] In MeCN. [e] See Ref. 6.

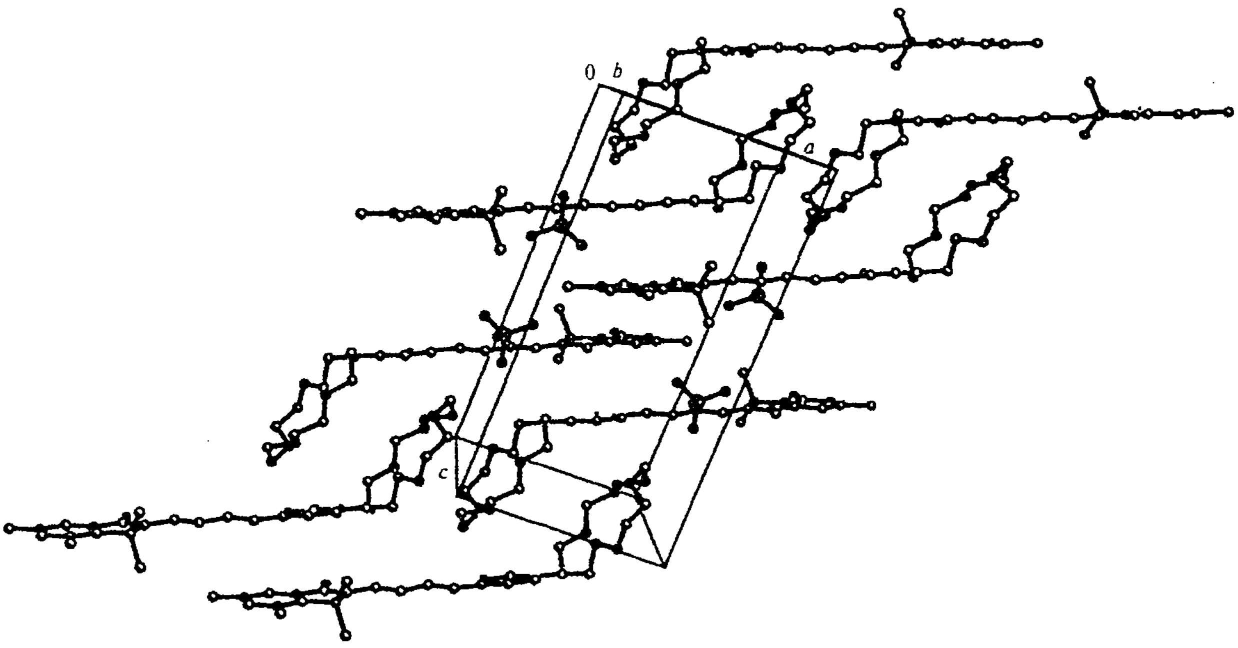

Fig. 2. Crystal packing of the structural units of *trans,trans*-**2a**.

with the possible participation of the lone electron pair of the N(1) atom in conjugation. The C(12)—C(13) (1.389(7) and 1.388(7) Å) and C(15)—C(16) (1.373(7) and 1.375(7) Å) bonds are shorter than the remaining four bonds in this ring (1.398(7)—1.421(7) Å in molecule **A** and 1.395(7)—1.418(7) Å in molecule **B**). The similar paraquinoid distribution of bond lengths, though somewhat less pronounced, was observed previously in the structure of *trans*-**1** (see Ref. 17). Like *trans*-**1**, the bonds at the N(1) atoms in *trans,trans*-**2a** have a planar configuration. The sum of the bond angles at this atom is 359.3° and 359.6° in **A** and **B**, respectively, while the C(11)—N(1) bond length (1.376(6) and 1.380(6) Å) corresponds to the standard bond length in the C_{Ar}—$N(C_R)_2$ fragment with the planar geometry of the NC_3 group (1.371(16) Å)[16] but is somewhat larger than the corresponding value in *trans*-**1** (1.369(2) Å). This indicates that the lone electron pair of the N(1) atom in *trans,trans*-**2a** is involved in conjugation with the chromophore to a lesser degree compared to *trans*-**1**.

The structural data made it possible to determine the extent of the chromophore in *trans,trans*-**2a**, which spans the chain bonds from the N(2) atom to the N(1) atom. In this connection, large hypsochromic shifts of the long-wavelength absorption bands in *trans,trans*-**2a** that occur upon addition of salts of alkali and alkaline-earth metal to solutions under study are attributable to the electron-withdrawing effect of the metal cation, which is bonded with the complex through the N(1) atom, on the degree of conjugation in the atomic chain of the chromophore. One would also expect that the constants of complexation of *trans,trans*-**2a** with metal cations are somewhat larger than those in the case of *trans*-**1** because in the latter case the lone electron pair is involved in conjugation with the chromophore to a greater extent.

The crown ether fragment in *trans,trans*-**2a** is inclined to the plane of the conjugated framework of the molecule (Fig. 2). The dihedral angle between the plane of the benzene ring and the mean plane through the heteroatoms of the crown ether fragment is 54.2° and 54.7° in **A** and **B**, respectively.

The conformations of the sequentially located X—C—C—X fragments (X = N or O) in the crown ether macrocycle (starting with the N(1)—C(1) bond) can be described as GTT GGT TGT TGG TGG in **A** and GTT GGT GGT TGT TGG in **B** (G = *gauche* and T = *trans*). In two independent cations of *trans,trans*-**2a**, the crown ether fragments have different conformations, both of them differing from that observed in *trans*-**1**.

The high conformational flexibility of the crown ether fragment has a profound effect on the formation of the crystal structure of *trans,trans*-**2a**. The fragment of the crystal packing of *trans,trans*-**2a** is shown in Fig. 2. In this crystal structure, the organic cations of the same type are arranged in stacks in a head-to-head rather than in a head-to-tail fashion, as distinguished from the crystals of *trans*-**1**. What the crystal packings of dyes *trans,trans*-**2a** and *trans*-**1** have in common is that they contain very loose channels formed by crown ether fragments of the molecules. The shortest interatomic distance between the H atoms in *trans,trans*-**2a** (2.7 Å) is larger than twice the van der Waals radius of the H atom (2.4 Å). The other distances between the H atoms of the adjacent molecules are larger than 3 Å. Apparently, both crystal structures are governed by two opposing tendencies. The first tendency consists of the formation of stacks of planar dye molecules, which provide the closest molecular packing. The second tendency lies in the fact that the crown ether fragment tends to retain conformational flexibility. These tendencies have to be taken into account in constructing models of self-assembly of molecules of this type to form supramolecular systems[1] in solutions or in films.

Electronic spectra and dark and photoinduced complexation of crown-containing butadienyl dyes

The absorption spectra of crown-containing butadienyl dyes *trans,trans*-**2a**—**e** in MeCN and their fluorescence spectra in EtOH are shown in Fig. 3. The introduction of the crown ether fragment into molecules of butadienyl dyes of the indolenine and benzothiazole series leads to small low-frequency shifts of the long-wavelength absorption band (in MeCN) and to an increase in the extinction coefficient of the dyes (see Table 6). In going from MeCN to EtOH, the long-wavelength absorption bands of dyes are shifted to the low-frequency region by $\Delta\nu$ = 250—550 cm^{-1}. This is typical of polymethine dyes and is apparently associated with an increase in the donor number of the solvent.[9] An increase in the electron-donating ability of the heterocyclic fragment of the dye in the CSD series generally leads to low-frequency shifts both of the long-wavelength band and of the fluorescence band and to an increase in the quantum yield of fluorescence (φ_f) (see Ref. 4). In our case, the replacement of the benzothiazolium moiety by the indoleninium fragment, which possesses substantially stronger electron-withdrawing properties, causes, on the contrary, a substantial bathochromic shift of the long-wavelength band, which is apparently due to nonaromaticity of the five-membered ring of the indoleninium group, unlike that in the benzothiazolium fragment. Previously, we have observed this effect in the case of CSD. As expected, the introduction of the second C=C double bond leads to substantial long-wavelength shifts of the absorption and fluorescence spectra (see Table 6). Apparently, the increase in φ_f observed in going from **2c** to **2a** and **2b** and from **2e** to **2d** is due to an increase in the volume and/or in the moment of inertia of the fragments of the molecule that undergoes isomerization.

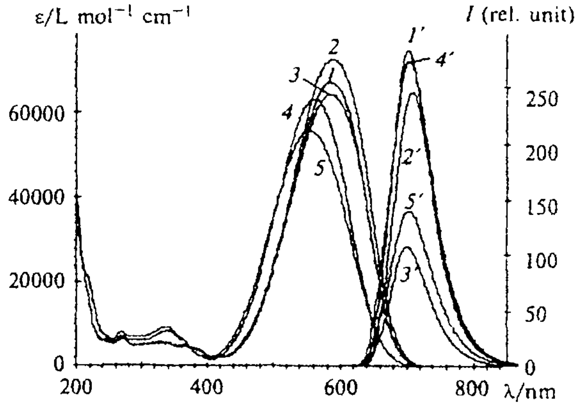

Fig. 3. Absorption spectra (*1*—*5*) in MeCN and fluorescence spectra (*1'*—*5'*) in EtOH of *trans,trans*-**2a** (*1*, *1'*), *trans,trans*-**2b** (*2*, *2'*), *trans,trans*-**2c** (*3*, *3'*), *trans,trans*-**2d** (*4*, *4'*), and *trans,trans*-**2e** (*5*, *5'*).

Addition of perchlorates of alkali (Li or Na) or alkaline-earth (Ca) metals to a solution of dye *trans,trans*-**2a** in MeCN led to a substantial ($\Delta\nu_a$ up to 5060 cm^{-1}) shift of the long-wavelength band and to a small ($\Delta\nu_f$ ~200 cm^{-1}) shift of the fluorescence spectrum to the high-frequency region (Table 7). The dependence of the absorption and fluorescence spectra of *trans,trans*-**2a** on the concentration of $Ca(ClO_4)_2$ is shown in Fig. 4. The equilibrium constants of complexation calculated with the use of the absorption spectra (K_a = [(*trans,trans*-**2a**) · M^{n+}]/[(*trans,trans*-**2a**)][M^{n+}], where [M^{n+}] is the concentration of the metal cations), the analogous constants calculated with the use of the fluorescence spectra (K_f) of the complexes with the stoichiometry of 1 : 1 (Scheme 2), the calculated values of the maxima of the long-wavelength absorption bands (λ_a) and of the fluorescence spectra (λ_f) of these complexes, and the values of the high-frequency shifts of the maxima of the long-wavelength bands in the absorption ($\Delta\nu_a$) and fluorescence ($\Delta\nu_f$) spectra of *trans,trans*-**2a** that occur upon complexation are given in Table 7.

Table 7. Spectral characteristics of the complexes of *trans,trans*-**2a,c** with H^+ and metal ions in MeCN

Compound	$\log K_a$ [L mol^{-1}]	$\log K_f$ [L mol^{-1}]	λ_a/nm	$\Delta\nu_a{}^a$/cm^{-1}	λ_f/nm	$\Delta\nu_f{}^a$/cm^{-1}	$\varepsilon_a \cdot 10^{-3}$ /L mol^{-1} cm^{-1}	$\varphi_f \cdot 10^{-2}$
2c · H^+	1.21	—	406	7360	—	—	47.2	<0.1
2a · H^+	2.18	—	408	7280	—	—	42.5	<0.1
2a · Li^+	1.96	1.87	543	1210	694	190	54.5	9.8
2a · Na^+	1.40	1.38	519	1970	699	30	47.1	9.1
2a · Ca^{2+}	2.28	2.09	450	5060	691	260	47.4	8.0
1 · Ca^{2+} [b]	—	—	410	—	590	—	30.0	—
			480—530 (sh)					

[a] $\Delta\nu_{a,f} = \nu_{a,f}(\text{complex}) - \nu_{a,f}(\text{ligand})$. [b] See Ref. 6.

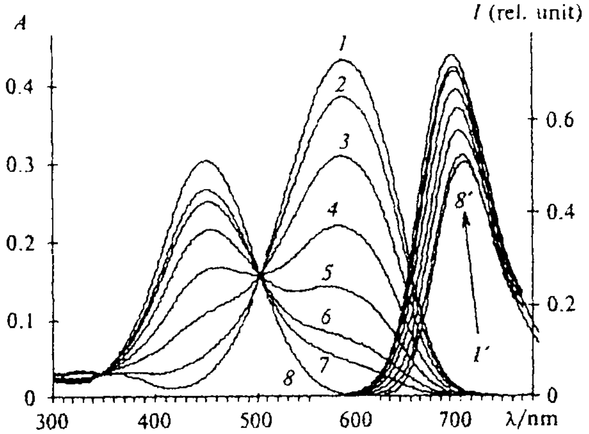

Fig. 4. Experimental (*1—7, 1'—7'*) and calculated (*8, 8'*) absorption (*1—8*) and fluorescence (*1'—8'*) spectra of *trans,trans*-**2a** (*1—7, 1'—7'*) and (*trans,trans*-**2a**) · Ca^{2+} (*8, 8'*) in MeCN at ~20 °C. The concentration of $Ca(ClO_4)_2$, C_M: 0 (*1, 1'*), $4.66 \cdot 10^{-4}$ (*2, 2'*), $1.23 \cdot 10^{-3}$ (*3, 3'*), $2.41 \cdot 10^{-3}$ (*4, 4'*), $4.50 \cdot 10^{-3}$ (*5, 5'*), $9.43 \cdot 10^{-3}$ (*6, 6'*), and $1.87 \cdot 10^{-2}$ mol L^{-1} (*7, 7'*). $C_L = 6.5 \cdot 10^{-6}$ mol L^{-1}.

Scheme 2

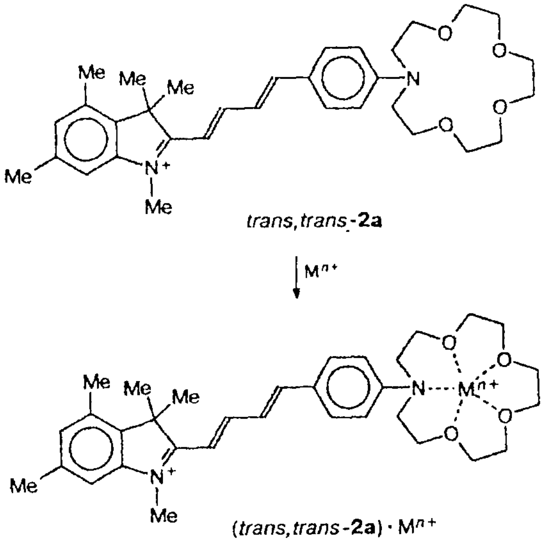

M^{n+} = Li^+, Na^+, Ca^{2+}

The excitation fluorescence spectra of *trans,trans*-**2a** are shifted to the high-frequency region by no less than 1410, 2600, and 5050 cm^{-1} upon additon of Li, Na, and Ca perchlorates with the concentrations $C_M = 5.73 \cdot 10^{-2}$, $21.5 \cdot 10^{-2}$, and $3.28 \cdot 10^{-2}$ mol L^{-1}, respectively. These shifts are similar to the analogous shifts of the long-wavelengths bands. By analogy with the CSD complexes studied previously (see Refs. **4—7**; in their spectra the positions of the maxima of the long-wavelength bands differ substantially, while the positions of the fluorescence maxima differ only slightly), it can be concluded that the photoinduced recoordination reaction proceeds in the complexes of *trans,trans*-**2a** with metal ions. This reaction involves the cleavage of the coordination bond between the metal cation and the N atom of the macrocycle and the displacement of the cation from the equilibrium position, which it occupies in the ground state (Scheme 3).

Scheme 3

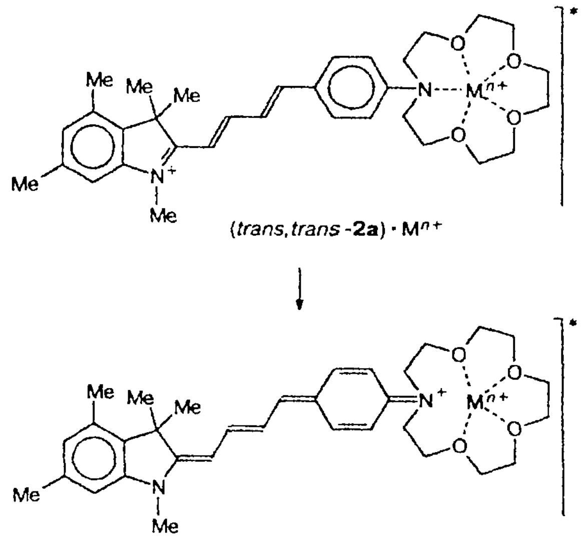

However, it should be noted that the absorption spectrum of (*trans,trans*-**2a**) · Ca^{2+} does not have a low-intensity band, which is observed in the case of (*trans*-**1**) · Ca^{2+} as a long-wavelength shoulder of the band with a maximum at 410 nm (see Ref. 6 and Table 7). This indicates that, unlike (*trans*-**1**) · Ca^{2+}, only one form of (*trans,trans*-**2a**) · Ca^{2+}, namely, the form containing the Ca^{2+}—N bond, is stable.

The recoordination reaction in the complexes of *trans,trans*-**2a** proceeds according to the intramolecular mechanism. This is confirmed by comparing the equilibrium constants K_a and K_f of the fluorescence spectra of *trans,trans*-**2a** and its complexes and the fluorescence spectra of *trans,trans*-**2a** and (*trans,trans*-**2a**) · Na^+ in the solid glassy butyronitrile matrix at 77 K. The close values of $\lg K_a$ and $\lg K_f$ indicate that dissociation of the complex in the excited state may be ignored. This is also evidenced by the higher value of φ_f of the product of photoinduced recoordination in a solution compared to φ_f of CBD and by the close values of the wavelengths of the maxima of the fluorescence spectra of *trans,trans*-**2a** and (*trans,trans*-**2a**) · Na^+ in the solid matrix at low temperature, where translation diffusion of the dye and the metal cation is impossible. This allows the conclusion that elimination of the metal ion from the cavity of the azacrown ether fragment, which has been proposed previously for complexes of merocyanine dye,[19] is not necessary for the photoinduced recoordination reaction to occur and this elimination does not occur in the case of CBD complexes.

$$K_a = \frac{[(trans,trans\text{-}\mathbf{2a})\cdot CF_3COOH]}{[(trans,trans\text{-}\mathbf{2a})][CF_3COOH]}$$

The value of K_a for protonation of *trans,trans*-**2a** with trifluoroacetic acid in MeCN is almost two orders of magnitude larger than the constant of protonation of *trans,trans*-**2c**. The difference in their basicity is apparently due to the participation of the O atoms of the crown ether fragment of *trans,trans*-**2a** in stabilization of the protonated N atom through intramolecular hydrogen bonding. The protonated forms of *trans,trans*-**2a,c** show no fluorescence in MeCN.

Complexation of *trans,trans*-**2a** with Li^+ affects the value of the shift of the long-wavelength band to a lesser degree than complexation with Na^+ (see Table 7). This is associated with the fact that Li^+ has a substantially smaller diameter than the size of the macrocycle cavity, forms, apparently, coordination bonds predominantly with the O atoms of the aza-15-crown-5 ether fragment, and, correspondingly, affects only slightly the conjugation between the N atom of the macrocycle and the chromophore.

The formation of complexes of *trans,trans*-**2a** with metal ions leads to a change in the quantum yield of fluorescence. The values of φ_f for the complexes with Li^+, Na^+, and Ca^{2+} ions are approximately twice as large as that observed for the initial dye. Generally, the opposite effect is observed for CSD[1] although there are exceptions to this rule.[5,6] Previously,[20] an increase in the quantum yield of fluorescence that was observed upon complexation of crown-containing styrylbenzodiazinone has been attributed to the fact that the metal cation hinders transition of the excited dye molecule to the twisted charge-transfer state. However, in the case of *trans,trans*-**2a** the situation may be complicated by the contribution of *trans—cis* photoisomerization to nonradiative deactivation of excitation.

Changes in the absorption and fluorescence spectra observed upon complexation can be partially associated with the salting effect. With the aim of estimating this effect, we measured the absorption and fluorescence spectra of dye *trans,trans*-**2c** in the presence of $Mg(ClO_4)_2$ (the Mg^{2+} cation has a higher surface charge density than other metal ions under consideration). It appeared that the absorption and fluorescence spectra of *trans,trans*-**2c** were changed only slightly in the presence of Mg^{2+} up to the concentration $C_{Mg} = 0.1$ mol L^{-1}. In this case, the extinction coefficient and the value of φ_f of *trans,trans*-**2c** increased by ~2% and ~15%, respectively; $\Delta\nu_a \approx 70$ cm^{-1} and $\Delta\nu_f \approx 0$ cm^{-1}. These data demonstrate that the salting effect may be ignored when considering the absorption and fluorescence spectra of *trans,trans*-**2a**.

We studied laser radiation of the synthesized butadienyl dyes *trans,trans*-**2a,b,d,e** upon excitation with the second harmonic of a ruby laser (λ = 347 nm). It was found that these dyes generate laser radiation in the 687—730-nm spectral region. The introduction of the crown ether fragment instead of the NMe_2 group into the dye molecule resulted in an increase in the efficiency of laser radiation (η) by a factor of ~10. The value of η increased by a factor of 1.3—2.3 upon complexation of butadienyl dyes *trans,trans*-**2a,b,d** with metal ions.

Therefore, we synthesized for the first time crown-containing butadienyl dyes bearing different heterocyclic fragments and crown ether fragments. The three-dimensional structure of the crown-containing butadienyl dye was studied for the first time. The results of our work reveal the effects of the nature of the heterocyclic and crown ether fragments, the temperature, and the medium on fluorescence and generation of dyes of the butadienyl series. This provides the basis for the targeted changes of their fluorescent parameters and the complex-forming ability with the use of synthetic approaches.

Experimental

The ^1H NMR spectra were recorded on Bruker AC-200p and Bruker AMX-400 spectrometers in $CDCl_3$ and DMSO-d_6 with Me_4Si as the internal standard. The chemical shifts were measured with an accuracy of 0.01 ppm. The spin-spin coupling constants were measured with an accuracy of 0.1 Hz. The IR spectra were recorded on a Shimadzu IR-470 spectrophotometer as KBr pellets. The mass spectra were obtained on a Varian MAT-311A instrument with direct inlet of the sample into the ionization zone; the energy of ionizing electrons was 70 eV. The course of the reactions was monitored by TLC on DC-Alufolien Kieselgel 60 F_{254} plates (Merck).

Crown-containing cinnamaldehydes were synthesized with the use of *N*-phenylaza-15-crown-5 ether purchased from Merck and *N*-phenylaza-18-crown-6 ether purchased from the Scientific and Technical Company "Physicochemical Institute of the National Academy of Sciences of Ukraine." Acetonitrile was successively distilled over $KMnO_4$, P_2O_5 (twice), and CaH_2 to remove admixtures and water. Ethanol was purified by boiling with 2,4-dinitrophenylhydrazine and concentrated HCl for 8 h followed by fractional distillation. Trifluoroacetic acid was dried by distillation from a mixture with sulfuric acid. The absorption spectra were measured on a Shimadzu UV-3100 spectrophotometer. The fluorescence spectra were recorded on an Elyumin-2M spectrofluorometer. The electronic fluorescence spectra were corrected for the spectral dependence of the sensitivity of the spectrofluorometer recording system. The quantum yield of fluorescence φ_f was determined by comparing the areas under the corrected spectra of the dye under study and of Cresyl Violet in ethanol (φ_f = 0.59)[21] on a PC-AT computer using the SPECTR program. The measurements were carried out at 77—296 K. The solutions of dyes were kept for 1 h to achieve complete complexation with metal perchlorates. The completion of the reaction was monitored using the absorption spectra. The equilibrium constants and the absorption and fluorescence spectra of the CBD complexes were calculated based on the global analysis of the series of the absorption and fluorescence spectra of CBD at various concentrations of metal perchlorate using the EQUILI program.

3-(4-Dimethylaminophenyl)propen-2-al (6c). A solution of $POCl_3$ (0.51 mL, 5.6 mmol) in anhydrous THF (10 mL) was added dropwise with stirring to a solution of *N*-methyl-*N*-phenylaminoacrolein **5** (0.75 g, 4.7 mmol) and *N,N*-dimethylaniline **7c** (0.59 mL, 4.7 mmol) in anhydrous THF (30 mL) at −10 °C. The reaction mixture was stirred at −10 °C for 2 h. Then hexane (100 mL) was added and the mixture was kept for 12 h. The resulting oil was separated and dissolved in MeOH (20 mL). A 10% Na_2CO_3 solution was added dropwise at 0 °C to pH 9. The resulting solution was extracted with benzene. The extracts were dried with $MgSO_4$ and concentrated. The residue was purified by column chromatography on SiO_2 (Kieselgel 60, 0.063—0.200 mm, Merck, a 5 : 1 benzene—AcOEt mixture as the eluent). Aldehyde **6c** was obtained as pale-yellow crystals in a yield of 0.39 g.

3-[4-(4,7,10,13-Tetraoxa-1-azacyclopentadecyl)phenyl]-propen-2-al (6a). A solution of $POCl_3$ (0.2 mL, 2.24 mmol) in anhydrous THF (10 mL) was added dropwise with stirring to a solution of *N*-methyl-*N*-phenylaminoacrolein (**5**) (0.32 g, 2 mmol) and *N*-phenylaza-15-crown-5 ether (**7a**) (0.68 g, 2.3 mmol) in anhydrous THF (10 mL) at −10 °C. The reaction mixture was stirred at −10 °C for 2 h and then at ~20 °C for 4 h. Then hexane (100 mL) was added and the reaction mixture was kept for 12 h. The resulting oil was separated and dissolved in MeOH (10 mL). A 10% Na_2CO_3 solution was added dropwise at 0 °C to pH 9. The resulting solution was extracted with benzene. The extracts were dried with $MgSO_4$ and concentrated. The residue was purified by column chromatography on SiO_2 (Kieselgel 60, 0.063—0.200 mm, Merck, AcOEt as the eluent). Aldehyde **6a** was obtained as pale-yellow crystals in a yield of 0.26 g. UV (MeOH), λ_{max}/nm: 250 (ε 10400), 389 (ε 35200). IR (KBr), ν/cm^{-1}: 1660 (C=O). MS, *m/z* (I_{rel} (%)): 349 (100), 230 (17), 173 (24), 160 (31), 132 (21), 131 (26), 98 (19), 73 (27), 70 (19), 57 (73), 55 (51).

3-[4-(4,7,10,13,16-Pentaoxa-1-azacyclooctadecyl)phenyl]-propen-2-al (6b). Compound **6b** was prepared analogously to **6a** from *N*-methyl-*N*-phenylaminoacrolein (**5**) and *N*-phenylaza-18-crown-6 ether (**7b**). Aldehyde **6b** was isolated as pale-yellow crystals. UV (MeOH), λ_{max}/nm: 251 (ε 9900), 391 (ε 36700). IR (KBr), ν/cm^{-1}: 1660 (C=O). MS, *m/z* (I_{rel} (%)): 393 (100), 216 (21), 204 (10), 160 (28), 158 (12), 131 (21), 103 (14), 102 (7), 86 (9), 58 (11), 57 (23).

Synthesis of dyes *trans,trans*-2a—e (general procedure). Compound **6a—c** (0.17 mmol), quaternary salt **3a,b** (0.15 mmol), pyridine (0.02 mL), and anhydrous EtOH (2 mL) were mixed in a flask equipped with a reflux condenser. The reaction mixture was refluxed for 18 h and cooled. The precipitate that formed was filtered off and recrystallized from EtOH. Dyes *trans,trans*-**2a—e** were obtained as nearly black crystals.

The principal physicochemical characteristics of the compounds synthesized and the parameters of their ^1H NMR spectra are given in Tables 1 and 2, respectively.

X-ray diffraction study of compound *trans,trans*-2a. Nearly black crystals of *trans,trans*-**2a** are triclinic, $a = 9.6338(1)$ Å, $b = 17.8750(2)$ Å, $c = 19.2270(1)$ Å, $\alpha = 100.087(1)°$, $\beta = 91.908(1)°$, $g = 90.604(1)°$, $V = 3257.53(5)$ Å^3, $d_{calc} = 1.291$ g cm^{-3}, $Z = 4$, space group $P\bar{1}$. The unit cell parameters and intensities of 11463 independent reflections were measured on an automated three-circle Siemens SMART CCD diffractometer (150.0(2) K, Mo-Kα radiation, graphite monochromator, ω scanning technique, the time per scan step was 30 s, the scan step was 0.3°) using a crystal of dimensions 0.30×0.30×0.20 mm.

The structure was solved by the direct method using the SHELXS-86 program package (see Ref. 22) and refined anisotropically by the full-matrix least-squares method based on F^2 using the SHELXL-93 program package (see Ref. 23). The positions of all hydrogen atoms were calculated geometrically and refined using the riding model with the temperature parameters B_{iso} half as much again as B_{eq} of the corresponding carbon atom. The final values of the *R* factors were as follows: $R = 0.0993$, $R_w = 0.2576$ for 10829 reflections with $I > 2\sigma(I)$. The experimental data were processed with the use of the Siemens SAINT program (see Ref. 24). The coordinates of nonhydrogen atoms are given in Table 5.

This work was financially supported by the Russian Foundation for Basic Research (Project Nos. 97-03-32968, 98-03-32355, and 98-03-33142), INTAS (Grant 95-IN-RU-237), and CRDF (Grant RC2-137).

References

1. S. P. Gromov and M. V. Alfimov, *Izv. Akad. Nauk, Ser. Khim.*, 1997, 641 [*Russ. Chem. Bull.*, 1997, **46**, 611 (Engl. Transl.)].
2. M. V. Alfimov and S. P. Gromov, in *Applied Fluorescence in Chemistry, Biology, and Medicine*, Eds. W. Rettig, B. Strehmel, S. Schrader, and H. Seifert, Springer-Verlag, Berlin, 1999, 161.
3. V. Balzani and F. Scandola, in *Comprehensive Supramolecular Chemistry*, Ed. J.-M. Lehn, Pergamon Press, New York, 1996, **10**, 687.
4. S. P. Gromov, O. A. Fedorova, M. V. Alfimov, S. I. Druzhinin, M. V. Rusalov, and B. M. Uzhinov, *Izv. Akad. Nauk, Ser. Khim.*, 1995, 2003 [*Russ. Chem. Bull.*, 1995, **44**, 1922 (Engl. Transl.)].
5. S. P. Gromov, A. A. Golosov, O. A. Fedorova, D. E. Levin, and M. V. Alfimov, *Izv. Akad. Nauk, Ser. Khim.*, 1995, 129 [*Russ. Chem. Bull.*, 1995, **44**, 124 (Engl. Transl.)].
6. E. N. Ushakov, S. P. Gromov, O. A. Fedorova, and M. V. Alfimov, *Izv. Akad. Nauk, Ser. Khim.*, 1997, 484 [*Russ. Chem. Bull.*, 1997, **46**, 463 (Engl. Transl.)].
7. S. I. Druzhinin, M. V. Rusalov, B. M. Uzhinov, M. V. Alfimov, S. P. Gromov, and O. A. Fedorova, *Proc. Indian Acad. Sci. (Chem. Sci.)*, 1995, **107**, 721.
8. S. P. Gromov, E. N. Ushakov, O. A. Fedorova, V. A. Soldatenkova, and M. V. Alfimov, *Izv. Akad. Nauk, Ser. Khim.*, 1997, 1192 [*Russ. Chem. Bull.*, 1997, **46**, 1143 (Engl. Transl.)].
9. A. A. Ishchenko, *Stroenie i spektral'no-lyuminestsentnye svoistva polimetinovykh krasitelei* [*Structures and Spectral Luminescence Properties of Polymethine Dyes*], Naukova Dumka, Kiev, 1994, 232 pp. (in Russian).
10. K. Kato, *IEEE J. Quantum Electron.*, 1980, **QE16**, 1017.
11. M. V. Bondar', N. A. Derevyanko, G. G. Dyadyusha, V. M. Zibarovskii, A. A. Ishchenko, O. V. Przhonskaya, Yu. L. Slominskii, A. L. Smirnova, E. A. Tikhonov, and A. I. Tolmachev, *Kvantovaya Elektronika*, 1984, **11**, 462 [*Sov. J. Quantum Electronics* 1984, **11** (Engl. Transl.)].
12. S. P. Gromov and Yu. G. Bundel', *Dokl. Akad. Nauk SSSR*, 1985, **281**, 585 [*Dokl. Chem.*, 1985 (Engl. Transl.)].
13. S. P. Gromov, M. V. Fomina, and M. V. Alfimov, *Izv. Akad. Nauk, Ser. Khim.*, 1993, 1625 [*Russ. Chem. Bull.*, 1993, **42**, 1561 (Engl. Transl.)].
14. J. C. Sauer, in *Organic Synthesis*, Ed. N. Raljohn, 1962, **4**, 813.
15. C. Jutz, *Chem. Ber.*, 1958, **91**, 850.
16. F. H. Allen, O. Kennard, D. G. Watson, L. Brammer, G. Orpen, and R. Taylor, *J. Chem. Soc., Perkin Trans. 2*, 1981, 1.
17. M. V. Alfimov, A. V. Churakov, Y. V. Fedorov, O. A. Fedorova, S. P. Gromov, R. E. Hester, J. A. K. Howard, L. G. Kuz'mina, I. K. Lednev, and J. N. Moore, *J. Chem. Soc., Perkin Trans. 2*, 1997, 2249.
18. F. H. Allen, J. E. Davies, J. J. Galloy, O. Johnson, O. Kennard, C. F. Wacrae, E. M. Mitchell, G. F. Mitchell, J. M. Smith, and D. G. Watson, *J. Chem. Inf. Comput. Sci.*, 1991, **31**, 187.
19. M. M. Martin, P. Plaza, N. Dai Hung, Y. H. Meyer, and B. Valeur, *Chem. Phys. Lett.*, 1993, **202**, 425.
20. L. Cazaux, M. Faher, A. Lopez, C. Picard, and P. Tisnes, *J. Photochem. Photobiol. A: Chem.*, 1994, **77**, 217.
21. J. E. Sabol and M. G. Rockley, *J. Photochem. Photobiol. A: Chem.*, 1987, **40**, 245.
22. G. M. Sheldrick, *Acta Crystallogr.*, 1990, **A46**, 467.
23. G. M. Sheldrick, *SHELXL-93. Program for the Refinement of Crystal Structures*, University of Göttingen, Germany, 1993.
24. *SAINT, Version 4.050, Siemens Analytical X-ray Instruments Inc.*, Madison, Wisconsin, USA, 1995.

Received April 14, 1998;
in revised form September 30, 1998